SERS of insecticides and fungicides assisted by Au and Ag nanostructures produced by laser techniques

P.A. Atanasov[1], N.N. Nedyalkov[2], Ru. Nikov[3], N. Fukata[4], W. Jevasuwan[5], T. Subramani[6], D. Hirsch[7], B. Rauschenbach[8]

[1,2,3]Institute of Electronics, Bulgarian Academy of Sciences, Tzarigradsko chaussee 72, Sofia 1784, Bulgaria
[4,5,6]International Center for Materials for NanoArchitectonics (MANA), National Institute for Materials Science (NIMS), 1-1 Namiki, Tsukuba 305-0044, Japan
[7,8]Leibniz Institute of Surface Modification (IOM), Permoserstrasse 15, D-04318 Leipzig, Germany

***Abstract*—** *This study deals with the use of laser techniques for preparation of advanced Au and Ag nanostructures on SiO_2 (001) substrates to be applied to high-resolution analyses, namely, surface enhanced Raman spectroscopy (SERS) analyses. The optical and morphological properties of the nanostructures are compared with those of the PLD thin films. The activity is tested of the structures fabricated as substrates for SERS covered by small quantities (usually applied in agricultural medicine) of the Aktara 25 BG (thiamethoxam) insecticide and the Dithane DG (mancozeb) fungicide. To the best of our knowledge, Raman spectra of Aktara 25 BG are presented for the first time. The study has a direct bearing on the human health and food quality by way of assisting the detection of small amounts or residue of harmful pollutants.*

***Keywords*— laser deposition and annealing, Ag and Au nanostructures, SERS, insecticide Aktara 25 BG, fungicide Dithane DG.**

I. INTRODUCTION

The properties of noble metallic nanostructures (NSs) have been the subject of considerable fundamental and technological interest. Metal nanoparticles (NPs) play an important role in scientific investigation and nanotechnology. As a result of the progress in nanotechnologies during the last two decades, nanosystems find nowadays application in many areas, such as chemistry, optics, biology, agriculture, medicine, microelectronics, etc. [1].

The excitation spectrum of noble metallic sub-wavelength structures is determined by its surface plasmon resonance. The energy of the plasmon resonance depends strongly on the shape and composition of the nanostructures. The tunability of the plasmon resonances of noble metallic NPs can be exploited to position the optical resonances at specific wavelength regions of interest and has led to a wide range of applications. The strong local electro-magnetic field enhancement accompanying the surface plasmon resonances has also been used to manipulate light-matter interactions, so that noble metallic sub-wavelength structures have been widely applied in surface enhanced Raman spectroscopy (SERS) [2,3]. The enhancement of the Raman signal may reach a factor of 10^8-10^{12} – the method is thus capable of detecting even a single molecule [2]. The increase of the Raman signal is a result of a local electromagnetic field enhancement in the vicinity of a structured surface due to the excitation of local and surface plasmons. In addition to their fundamental importance, plasmonic nanostructures are receiving a great deal of attention for their potential applications in areas such as sub-wavelength waveguides, optical nanoantennas, photovoltaic technology for efficient light coupling into solar cells, metamaterials, chemical and biological sensing, and biomedical applications [4-7].

Among the physical techniques, laser-based syntheses of nanomaterials have constituted a continuously growing field of research. In particular, pulsed laser ablation of solid targets in different environments, e.g. vacuum, background gas or liquid, has become an attractive method for the generation of NPs and deposition of NPs-assembled materials [8]. Among the successfully applied techniques one can mention the ns-laser deposition of thin metal films and the post-deposition structuring [9-13]. The nanostructuring of thin metal films by excimer laser pulses has been introduced as a technique for production of nanoparticles on different substrates [12,14]. The fragmentation of the metal surface into nanosized droplets during the melting is due to the poor wetting between the substrate and the liquid phase [15]. Moreover, femtosecond laser nanostructuring of silicon-based SERS substrates has also been reported [14,16].

Au and Ag NSs produced by laser methods have been used successfully in SERS analyses. Thus, an enhancement has been observed of the R6G Raman spectrum on Au nanocolumns formed by off-axis pulsed laser deposition (PLD). Concentrations of R6G as low as 1 nM [3] have been measured and a maximum enhancement higher than 10^5 has been achieved.

SERS has been used for trace analyses and detection of residue of different organophosphorous pesticides and insecticides [17-22] by employing various nanostructures, such as a solution of 100 nm Ag nanocubes [18] and a Klarite Au-coated SERS-active substrate [19-21]. The SERS analyses have been compared with the traditional analyses, as chromatography, fluorescence polarization immunoassay, multi-enzyme inhibition assay, and biosensors. Although the traditional methods can be used to detect trace amounts of pesticides, they are time-consuming, labor-intensive and expensive, which makes them less attractive and limiting to a certain extent the laboratory, real-time, and field detection [19].

Among the large variety of pesticides, dimethoate is a widely-studied substance. The lowest concentration registered has been 5÷10 μg mL^{-1} using confocal Raman micro-spectrometry with Klarite substrates [19]. Generally, a low concentration at about 10^{-6} can be detected.

The Dithane DG fungicide (mancozeb as an active substance) and the Aktara 25 BG insecticide (thiamethoxam as an active substance) are among the chemicals used extensively in agricultural medicine as protective substances for vegetables, fruits, crops etc. The fungicides from the dithiocarbamate group, as thiram, ferbam, ziram, metiram and zineb, have been widely studied in different SERS configurations using Au or Ag NSs [23-27]. Moreover, chemically produced gold nanorods have also been used as active SERS substrates for detection of ultra-low levels of fungicides from the dithiocarbamate group, i.e. thiram, ferbam and ziram [28]. Limits of detection as low as several nM have been achieved depending on the type of material tested. Furthermore, recording of Fourier transform Raman and surface-enhanced Raman spectra of a silver colloid of the mancozeb dithiocarbamate fungicide has been reported [29]; a slight decomposition has been observed of this material because of a metal exchange with the silver on the surface. As for the insecticide Aktara 25 BG (thiamethoxam), to the best of our knowledge no SERS study has been reported.

The aim of this paper is to describe a study on and the results of the development of laser technologies for formation of advanced Ag and Au nanostructures (NSs) by annealing PLD films on quartz. The as-produced NSs were used as active substrates for high-resolution analyses (SERS) to detect the Dithane DG fungicide and the Aktara 25 BG insecticide. Two types of concentrations of the two materials were analyzed and compared – low, as in routine agricultural use, and high, as offered on the market. The SERS spectra of Au and Ag NPs-covered areas and films were compared with the Raman spectra taken from high concentrations deposited directly on glass.

II. EXPERIMENTAL

2.1 Ag and Au active substrates synthesizing

The Ag or Au nanostructures were fabricated by means of a laser-based technique. As a first step, approximately 100-nm thick films were deposited by a standard PLD on 10×10 mm quartz (001) substrates at room temperature in vacuum (ambient pressure of ~10^{-3} Pa) using a THG Nd:YAG laser (Lotis TII) operating at λ = 532 nm at a repetition rate of 10 Hz with a pulse duration of 12 ns. The targets used were Au or Ag (both of 99.99 % purity, Alfa Aesar). The laser radiation (fluence of 1.5 J/cm^{-2}) was focused on the surface of the targets by a lens with a focal distance of 20 cm. The second step, i.e. producing the NPs, consisted of annealing the as-prepared films by a single pulse of the same laser wavelength with a fluence of 0.3 J/cm^2 incident on an area on the film with a diameter of ~4 mm, again in vacuum at room temperature. The as-prepared active samples were subjected to μ-Raman analyses.

2.2 Materials and Instrumentation

The Aktara 25 BG insecticide (Syngenta, Switzerland) and the Dithane DG fungicide (Indofil Industries Limited, India) were purchased from a specialized agricultural drugstore. The in-stock standard concentrations of the active chemicals are as follows: thiamethoxam $C_8H_{10}ClN_5O_3S$ in Aktara 25 BG is 250 g/kg (i.e., ¼ of the entire mass); and mancozeb $(C_4H_6MnN_2S_4)_x(Zn)_y$ in Dithane DG, 750 g/kg (i.e. ¾). In fact, mancozeb is a combination of two dithiocarbamates – maneb and zineb. Maneb is a polymeric complex of manganese with ethylene bis (dithiocarbamate) anionic ligand and zineb is the same, but with the manganese substituted by zinc. Figs. 1 a and b present the chemical structures of thiamethoxam and mancozeb, respectively.

Two drops of aqueous solution of each of the analytes, at the concentrations summarized in Table 1, were deposited on the Au and Ag active samples (the films and NPs sections). The samples were then dried at 50 ^oC. For comparison with the properties of the active substrates prepared, a drop of each of the analyte solutions at their highest concentrations (as obtained from stock) was deposited on a glass substrate and dried under the same conditions for μ-Raman analyses. In all cases, the areas on the substrates covered by the dried analytes had a diameter of ~4 mm, i.e. ~12 mm^2.

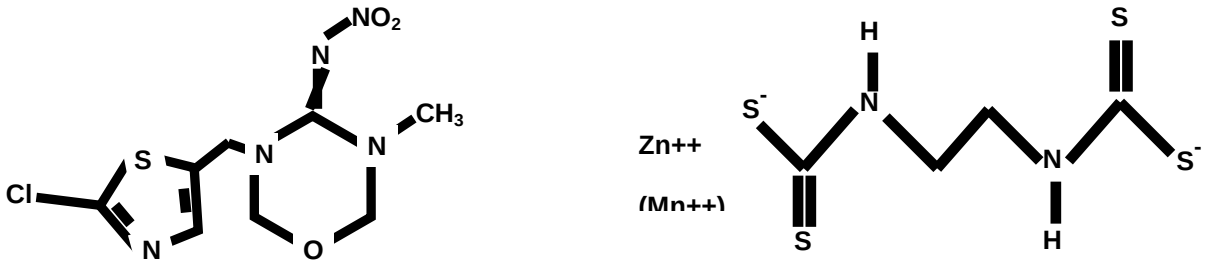

FIG. 1 CHEMICAL STRUCTURE OF: A) thiamethoxam; AND B) mancozeb (maneb + zineb).

TABLE 1
SUMMARIZED DESCRIPTION OF THE TESTED CHEMICALS AND THEIR CONCENTRATION

Name of the product studied	Active Chemical	Analyte, deposited on film or NPs areas	Analyte, deposited on glass	On sale
Insecticide Aktara 25	thiamethoxam	75 $\mu g \cdot mL^{-1}$ active substance; 0.26 mM	12.5 $g \cdot L^{-1}$ active substance; 43 mM	Powder; active substance 250 g/kg
Fungicide Dithane DG	mancozeb	0.75 $mg \cdot mL^{-1}$ active substance; 2.8 mM	37.5 $g \cdot L^{-1}$ active substance; 0.14 M	Powder; active substance 750 g/kg

The morphology of the samples was observed by scanning electron microscopy using a SU 8000 FE-SEM (Hitachi, Japan) and a FE-SEM (Zeiss Ultra55, Gemini) microscopes. The optical properties of the thin films and the NPs areas were measured by an optical spectrophotometer (Jasco V-670, Japan). The Raman spectra were obtained by an RMS-310 μ-Raman spectrometer (Photon Design, Japan). It uses an excitation power of 0.5 mW (image dimension of ~1 μm^2) at a wavelength of λ = 532 nm and has a resolution of 0.2 cm^{-1}.

III. RESULTS AND DISCUSSIONS

3.1 Morphological and optical properties of the Ag and Au substrates

The morphology of the samples was observed and analyzed by FE-SEM. Figs. 2 a-d present SEM images of the Ag and Au films and NPs arrays, respectively. As is evident, the Ag film was much flatter than the Au one. The insets in Figs. 2 a and d display histograms of the Ag and Au NPs size distributions evaluated by counting 500 particles. One can see that the Au NPs size distribution was quite narrow with a maximum at ~22 nm. Additionally, areas where the Au NPs had been completely evaporated were present, because of "hot spots" in the laser-beam energy distribution (Fig. 2 d). The Ag NPs size distribution (see inset in Fig. 2 b) had two maximums – one at ~10 nm corresponding to the smaller NPs, and second one at 30 ÷ 55 nm, corresponding to the larger NPs.

The optical properties of the Ag and Au films, as well as of the nanoparticles areas, were also studied. Figs. 3 a-d show the transmission spectra of the samples presented in Fig. 2. As is seen in Fig. 3, the plasmon resonance was very well pronounced in both cases, i.e. the Ag and Au NPs areas. However, it was much stronger and narrower in the case of Ag NPs (Fig. 3 b). It is worth noting that a plasmon resonance was also achieved in the case of the Ag film (Fig. 3 a); it had the same intensity as that in the Ag NPs area (Fig. 3 b), but was much wider. In what regards the Au film, the plasmon resonance was very shallow. Further, the plasmon resonance appeared at 525 nm for the Ag films and was shifted towards the shorter wavelengths, namely, 438 nm, for the Ag NPs. In the cases of the Au NPs and films, the respective values were 566 nm and ~681 nm. We assume that the features described above could be attributed to the characteristics of the structures explored.

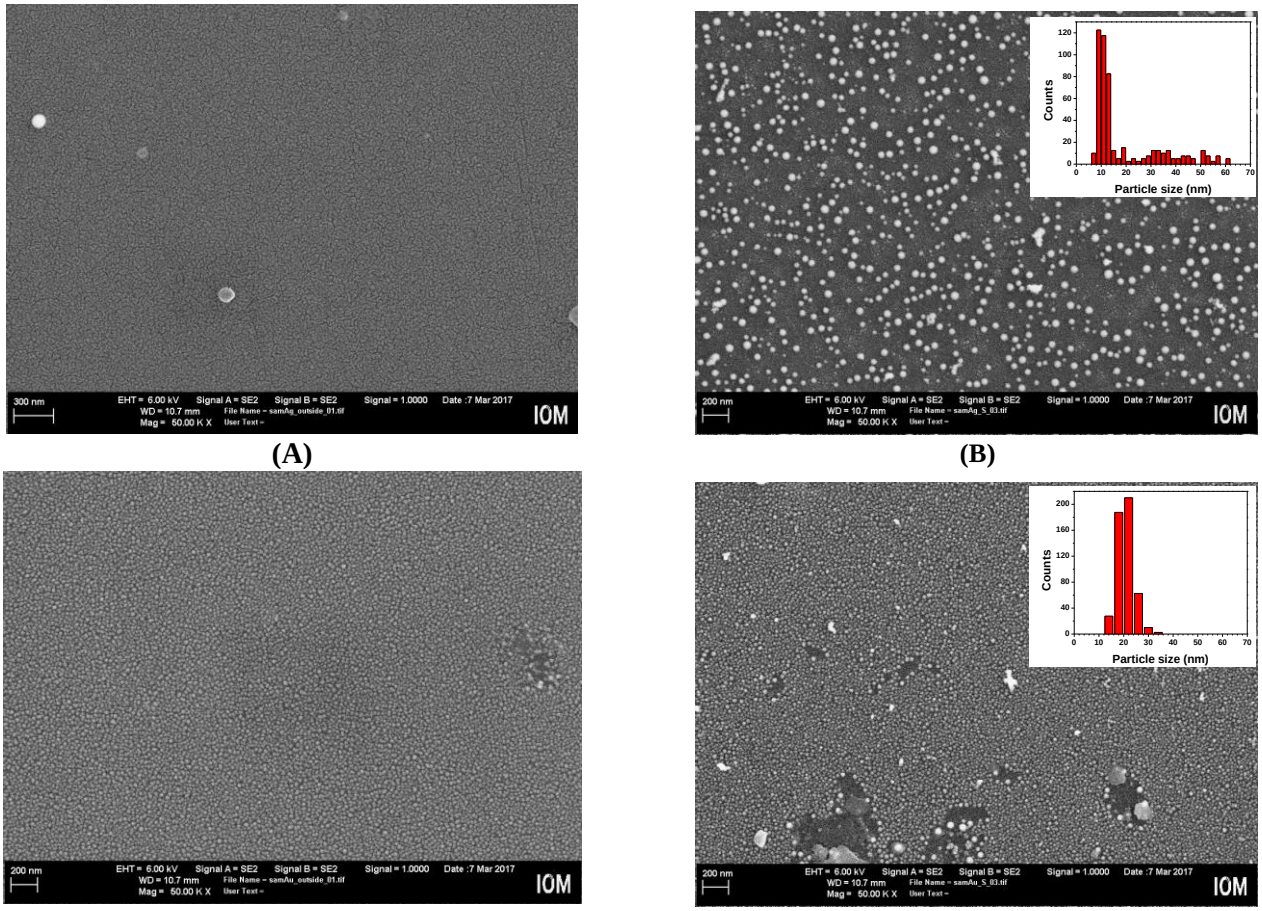

(A) (B)

(C) (D)

FIG. 2 Fe-SEM IMAGES OF: A) AG film; B) Ag NPs area; C) Au film; D) Au NPs AREA.

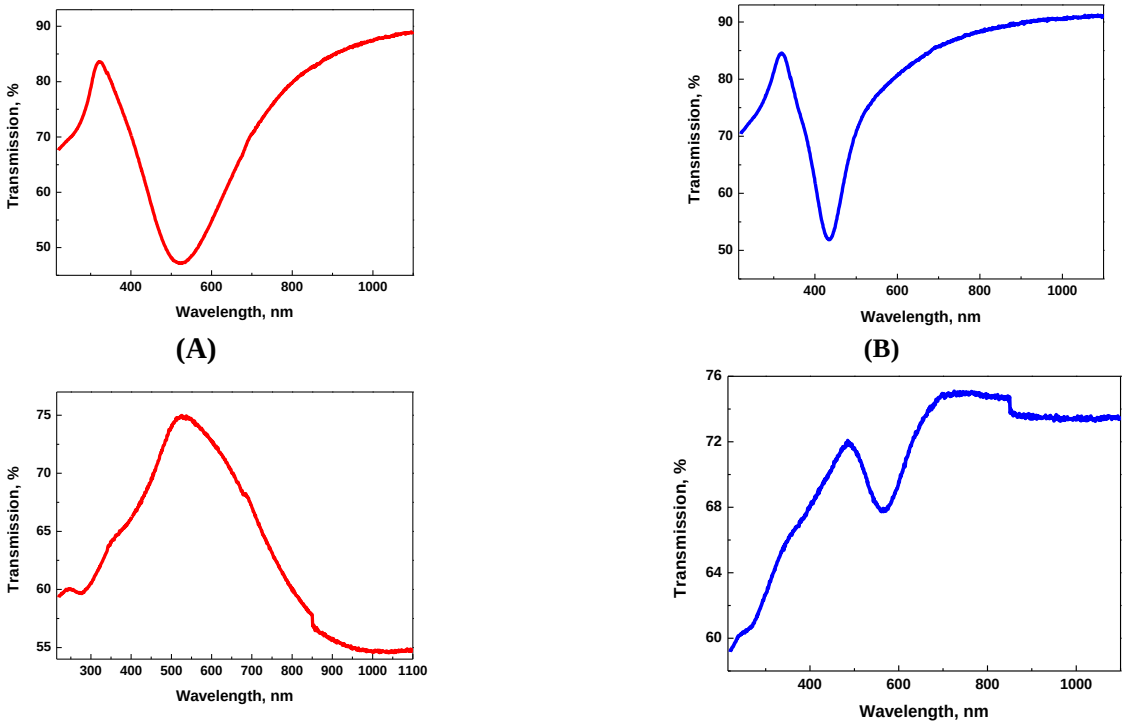

(A) (B)

(C) (D)

FIG. 3 TRANSMISSION SPECTRA OF: A) AG film; B) Ag NPs area; C) Au film; D) Au NPs.

3.2 SERS of Aktara and Dithane

The analytes in the active Ag and Au substrates (films and NPs areas) and the samples on glass were examined by μ-Raman spectrometry. Figs. 4 a-c present μ-Raman spectra of Aktara (thiamethoxam). As is seen, several strong peaks were detected from the Ag NPs area, while the Ag film gave rise to some shallow peaks. Additionally, several very week and broad peaks were observed when analyte with a higher concentration (more than two orders of magnitude) was deposited on the glass substrate. The parameters of the SERS peaks observed originating from the Ag NPs and the Ag film and the μ-Raman peaks recorded from the glass substrates are summarized in Table 2. To the best of our knowledge, a SERS study of the Aktara insecticide (thiamethoxam) is reported for the first time. The strongest peaks in the SERS spectra arising from the Ag NPs sample were located between 840 cm^{-1} and 1238 cm^{-1}. Additionally, peaks at 545 cm^{-1}, 583 cm^{-1} and 590 cm^{-1} of intermediate intensity could be seen. According to Nicholas et al. [30], who studied other structurally related halogenated (Cl) pesticides, several peaks below 600 cm^{-1} can be ascribed to the C-Cl linkage. Moreover, the activity between 600 cm^{-1} and 1600 cm^{-1} is characteristic for hydrocarbons. The peak at 1619 cm^{-1} can be related to a distortion of the benzene-type ring.

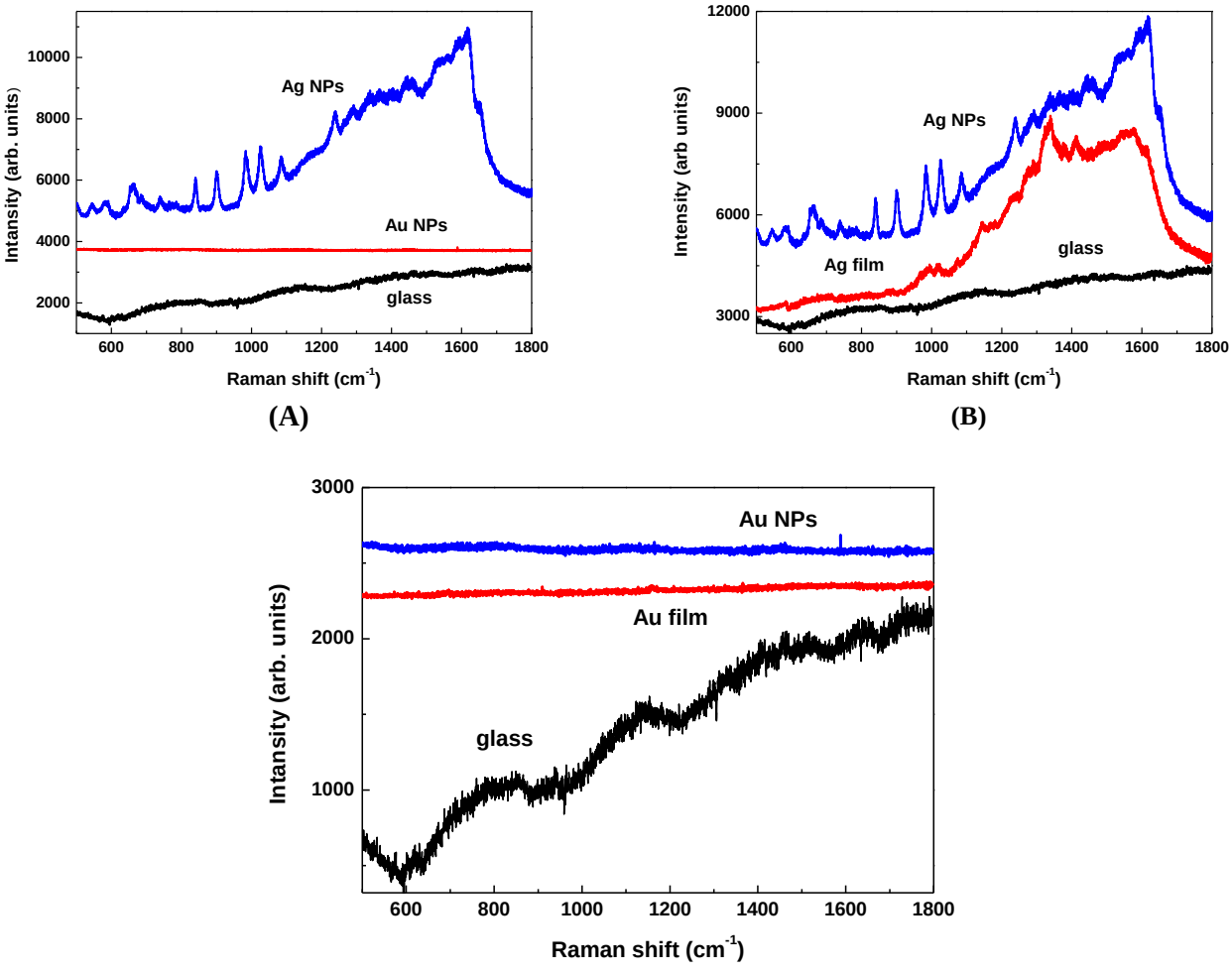

FIG. 4 μ-RAMAN SPECTRA OF AKTARA 25 (thiamethoxam) DEPOSITED ON: A) Ag and Au NPs and glass; B) Ag NPs and Ag film and glass; C) Au NPs and Au film and glass. Note that the concentration of the analyte deposited on glass is much higher compared to that deposited on Ag, Au films or NPs areas – see Table 1.

TABLE 2
SUMMARY OF THE VIBRATION MODES OBSERVED (cm^{-1}) of Aktara 25 (thiamethoxam). Relative intensity: vs – very strong; s – strong; m – middle; w – weak; vw – very weak; vwb – very week and broad.

SERS Ag NPs, cm^{-1}	SERS Ag film, cm^{-1}	μ-Raman spectrum, Glass, cm^{-1}
545, m	-	-
583, m	583, w	576, vwb
590, m	-	-
634, vw	634, vw	629, vwb
654, 663, m	663, vw	-
684, w	684, vw	-
738, w	-	-
840, vs	-	-
901, vs	-	-
983, vs	992, vw	-
1026, vs	1026, vw	-
-	1074, w	-
1084, s	-	-
-	1143, w	1144, vwb
1238, s	1238, vw	-
1290, w	1290, w	-
1339, w	1339, s	-
1366, vw	-	-
1413, vw	1413, m	1413, vwb
1443, w	1443, vw	-
1458, w	1458, vw	1458, vwb
1593, vw	-	-
1619, m	1619, w	-
1651, w	-	-

Regarding the results obtained, we did not reach the lower limit of detection. However, it is evaluated to be <6 ng of Aktara (thiamethoxam), as a result of the enhancement caused by the plasmon resonance in Ag NPs.

Au and Ag NPs, thin films and glass samples were also used for μ-Raman spectrometry analyses of the Dithane DG fungicide. Figs. 5 a-c show μ-Raman spectra of Dithane DG (mancozeb). As is seen, the enhancement in the case of Ag NPs was slightly higher than that of the Au NPs, while the Ag and Au films' SERS spectra had the same bands with a reduced intensity. It is worth noting that some shallow peaks appeared in the Raman spectrum when Dithan DG was deposited on glass. However, the concentration of the analyte there was much higher – more than three orders of magnitude (see Table 1). The characteristics of the SERS spectra originating from the Ag and Au NPs, the Ag and Au films, and the μ-Raman spectra of the glass substrate samples, are summarized in Table 3. The salient parameters of the Fourier transform Raman and SERS spectra (denoted by an asterisk) of mancozeb on a Ag colloid from Ref. [29] are also given for comparison. As is seen (Fig. 5 a and Table 3), the strongest six lines in the Ag NPs and Au NPs SERS spectra were: 603 cm^{-1}, 665 cm^{-1}, 942 cm^{-1}, 1350 cm^{-1}, 1438 cm^{-1} and 1514 cm^{-1}; the line at 1286 cm^{-1} was of intermediate intensity. They completely coincided with those reported in Ref. [29]. However, they were present in the Fourier transform Raman spectrum and missing in the SERS. The authors connect this effect with the degradation of the mancozeb on the Ag surface into the colloid used. In contrast, in our case the analyte was in a solid form on the surface of the active substrates, so that it probably did not degrade sufficiently. This was why the bands observed by us were visible in the SERS spectra with a high intensity. It is also worth noting that all seven bands, but with a lower intensity, were present in the μ-Raman spectrum of the analyte deposited on glass, or in the Ag and Au films' SERS spectra. The enhancement in the case of the Au film was very weak, as illustrated by the shallow plasmon resonance recorded (Fig. 3 c).

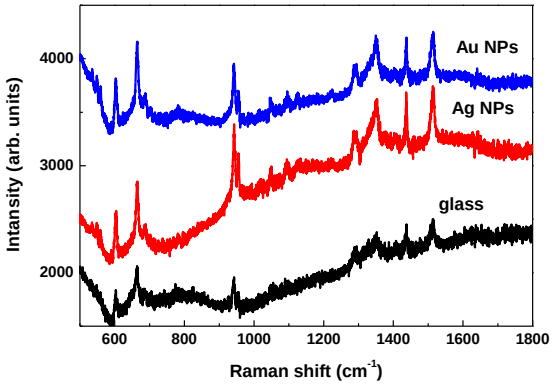

(A)

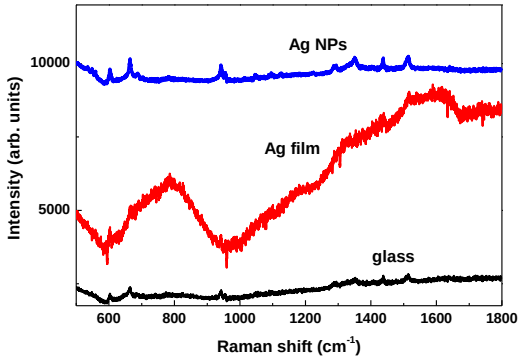

(B)

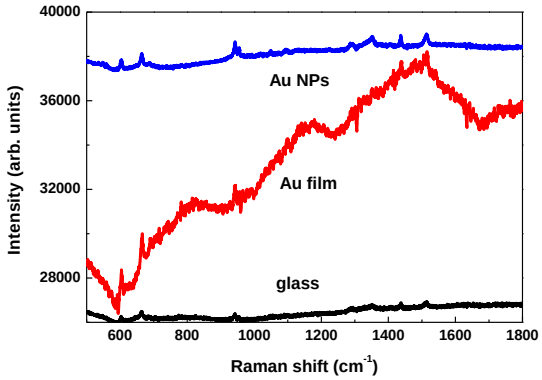

(C)

FIG. 5 μ-Raman spectra of Dithane DG (mancozeb) deposited on: A) Ag and Au NPs and glass; B) Ag NPs and Ag film and glass; C) Au NPs and Au film and glass. Note that the concentration of the analyte deposited on glass is much higher – see Table 1.

TABLE 3

SUMMARY OF THE VIBRATION MODES OBSERVED (cm^{-1}) of Dithane DG (mancozeb). Relative intensity: vs – very strong; s – strong; m – middle; w – weak; vw – very weak. All bands given in the last column are recorded by Fourier transform Raman spectroscopy; those marked by * are SERS [29].

SERS Ag NPs, cm^{-1}	SERS Ag film, cm^{-1}	SERS Au NPs, cm^{-1}	SERS Au film, cm^{-1}	μ-Raman spectrum, Glass, cm^{-1}	Ref. [29]
536, w	536, vw	536, vw	-	536, vw	-
546, w	-	546, vw	-	546, vw	-
560, w	560, vw	560, vw	-	560, vw	-
603, s	603, m	603, s	603, w	604, m	603, s
665, vs	665, w	665, vs	666, w	665, m	665, vs
689, w	689, vw	689, w	-	689, vw	-
783, vw	783, vw	783, vw	783, vw	783, vw	-
942, vs	942, m	942, vs	943, vw	942, m	945, vs
953, m	953, w	953, w	-	953, w	954, m*
1048, w	1048, w	1048, w	-	1048, vw	1051, m
1095, w	1095, vw	1095, w	-	1095, vw	-
1286, 1293, m	1286, vw	1286, 1293, m	-	1286, 1293, w	1292, s; 1282, m*
1350, vs	-	1350, s	-	1350, w	1351, s
1438, vs	1438, w	1438, vs	1438, w	1438, m	1438, s
1514, vs	1514, m	1514, s	1515, w	1514, m	1515, s

Based on the above results, several vibrations could be identified in the SERS spectra. The strong bands in the 600-700 cm^{-1} region, i.e. 603 cm^{-1} and 665 cm^{-1}, can be attributed to the different interactions of Zn and Mn with the CSS group [29]. The most intensive bands at 1514 cm^{-1} and 1438 cm^{-1} can be attributed to the (C=N) stretching coupled with deformation (NH) and (CH_2) vibrations [24,29]. The band monitored at 1286 cm^{-1} having intermediate intensity is probably connected to the NH motion [29]. Moreover, several peaks between 900 cm^{-1} and 1050 cm^{-1}, including the strongest bands at 942 cm^{-1} and 1048 cm^{-1}, correspond possibly to the stretching (C=S) motion. It could also be affected by the simultaneous presence of the bidentate and monodentate complex on the Ag or Au surfaces of the active substrates [29].

Finally, the limit of mancozeb detection was evaluated to be <60 ng for the Ag and Au NPs. However, the μ-Raman and SERS spectra indicated that this was not the lowest possible detection limit.

IV. CONCLUSION

The results obtained can be summarized as follow:

- Laser annealing of Au and Ag films on quartz substrates resulted in areas containing nanoparticles. The size of the Au NPs exhibited a quite narrow distribution with a maximum at ~22 nm; that of the Ag NPs was much broader with two maximums at ~10 nm and 30÷55 nm. A plasmon resonance was very well pronounced in both cases, but was much stronger in the case of Ag NPs. Additionally, a plasmon resonance with the same intensity as for the Ag NPs, although much wider, was also seen in the case of Ag films;

- To the best of our knowledge, for the first time a strong enhancement of the μ-Raman spectra was detected in the case of Aktara 25 BG deposited on the Ag NPs area caused by plasmon resonance in Ag NPs; thus, the minimum detectable Aktara (thiamethoxam) amount was estimated to be <6 ng.

- A strong enhancement of the μ-Raman spectra was registered in the case of Dithane DG deposited on Au NPs and Ag NPs areas, as compared with the case of Dithane DG deposited on glass, its concentration being much higher in the latter case notwithstanding. The limit of detection of mancozeb achieved based on μ-Raman SERS was evaluated to be <60 ng for Ag NPs or Au NPs, although there were indications that this is not the lowest limit possible.

Further improvement of the active substrates is needed in order to increase the sensitivity of the SERS analyses.

The experimental results reported are very promising and demonstrate a great potential for application as an additional and competitive method for analyses compatible with the existing chemical methods. Moreover, suitable and enhanced Ag or Au nanostructures of improved properties must be produced to improve the interaction with such molecules. This will be the subject of further investigations aimed at obtaining the higher sensitivity required for SERS analytical applications.

ACKNOWLEDGEMENTS

The authors acknowledge financial support from the projects DNTS 01/1 funded by the Bulgarian National Science Fund. P. Atanasov highly acknowledges financial support from JSPS under contract JSPS Fellow ID No. S16152.

REFERENCES

[1] "Recent Advances in Nanoscience and Technology", S. K. Bajpai and M. M. Yallapu (Eds), Bentham Sci. Pub., 2009.

[2] S. Nie and S. R. Emory, Probing single molecules and single nanoparticles by surface-enhanced Raman scattering, Science, vol. 275, pp. 1102-1106, 1997.

[3] T. Sakano, Y. Tanaka, R. Nishimura, N. N. Nedyalkov, P. A. Atanasov, T. Saiki, and M. Obara, Surface enhanced Raman scattering properties using Au-coated ZnO nanorods grown by two-step, off-axis pulsed laser deposition, J. Phys. D: Appl. Phys., vol. 41 (23), 235304, 2008.

[4] D. Pissuwan, S. M. Valenzuela, and M. Cortie, Therapeutic possibilities of plasmonically heated gold nanoparticles, Trends Biotechnol., vol. 24 (2), pp. 62-67, 2006.

[5] X. Huang, I. H. El-Sayed, W. Qian, and M. A. El-Sayed, Cancer cell imaging and photothermal therapy in the near-infrared region by using gold nanorods, J. Am. Chem. Soc., vol. 128, pp. 2115-2120, 2006.

[6] W. J. Cho, Y. Kim, and Y. K. Kim, Ultrahigh-density array of silver nanoclusters for SERS substrate with high sensitivity and excellent reproducibility, ACS Nano, vol. 6 (1), pp. 249-255, 2012.

[7] M. J. Beliatis, S. J. Henley, and S. R. P. Silva, Engineering the plasmon resonance of large area bimetallic nanoparticle films by laser nanostructuring for chemical sensors, Opt. Lett., vol. 36, pp. 1362-1364, 2011.

[8] S. Besnier and M. Meunier, in "Laser precision microfabrication" edited by K. Sugioka, M. Meunier, and A. Piqué, Springer Series in Materials Science Chap., Springer-Verlag Berlin, Chap. 7, 135, 2010.

[9] J. Bischof, D. Scherer, S. Herminghaus, and P. Leiderer, Dewetting modes of thin metallic films: nucleation of holes and spinodal dewetting, Phys. Rev. Lett., vol. 77 (8), 1536, 1996.

[10] M. N. Ashfold, F. Claeyssens, G. M. Fuge, and S. J. Henley, Pulsed laser ablation and deposition of thin films, Chem. Soc. Rev., vol. 33 (1), pp. 23-31, 2004.

[11] A. Pereira, A. Cros, P. Delaporte, S. Georgiou, A. Manousaki, W. Marine, and M. Sentis, Surface nanostructuring of metals by laser irradiation: effects of pulse duration, wavelength and gas atmosphere, Appl. Phys., vol. A 79, pp. 1433-1437, 2004.

[12] S. J. Henley, J. D. Carey, and S. R. P. Silva, Metal nanoparticle production by pulsed laser nanostructuring of thin metal films, Appl. Surf. Sci., vol. 253, pp. 8080-8085, 2007.

[13] P. A. Atanasov, N. N. Nedyalkov, A. Og. Dikovska, Ru. Nikov, S. Amoruso, X. Wang, R. Bruzzese, K. Hirano, H. Shimizu, and M. Terakawa, Noble metallic nanostructures: preparation, properties, applications, J. of Phys.: Conf. Ser., vol. 514, 1, 012024, 2014.

[14] S. J. Henley, J. D. Carey, and S. R. P. Silva, Laser-nanostructured Ag films as substrates for surface-enhanced Raman spectroscopy, Appl. Phys. Lett., vol. 88, 081904, 2006.

[15] S. J. Henley, J. D. Carey, and S. R. P. Silva, Pulsed-laser-induced nanoscale island formation in thin metal-on-oxide films, Phys. Rev., vol. B 72, 195408, 2005.

[16] E. Diebold, N. Mack, S. Doorn, and E. Mazur, Femtosecond laser-nanostructured substrates for surface-enhanced Raman scattering, Langmuir, vol. 25, 1790, 2009.

[17] L. Guerrini, S. Sanchez-Cortes, V. L. Cruz, S. Martinez, S. Ristori, and A. Feis, Surface-enhanced Raman spectra of dimethoate and omethoate, J. of Raman Spectroscopy, vol. 42 (5), pp. 980-985, 2011.

[18] J. C. S. Costa, R. A. Ando, A. C. Sant'Ana, and P. Corio, Surface-enhanced Raman spectroscopy studies of organophosphorous model molecules and pesticides, Phys. Chem. Chem. Phys., vol. 14 (45), pp. 15645-15651, 2012.

[19] Y. Liu, B. Ye, C. Wan, Y. Hao, Y. Lan, and A. Ouyang, Rapid quantitave analysis of dimethoate pesticide using surface-enhanced Raman spectroscopy, Am. Soc. of Agricultural and Biological Engineers, vol. 56 (3), pp. 1043-1049, 2013.

[20] Yande Liu and Tao Liu, Determination of pesticide residues on the surface of fruits using micro-Raman spectroscopy, Intern. Federation for Information Processing AICT, vol. 347, pp. 427-434, 2011.

[21] Bin Liu, Peng Zhou, Xiaoming Liu, Xin Sun, Hao Li, and Mengshi Lin, Detection of pesticides in fruits by surface-enhanced Raman spectroscopy coupled with gold nanostructures, Food Bioprocess Technol., vol. 6, pp. 710-715, 2013.

[22] P. X. Zhang, Xiaofang Zhou, Y. S. Andrew, and Cheng Yan Fang, Raman spectra from pesticides on the surface of fruits, J. of Phys.: Conf. Ser., vol. 28, pp. 7-11, 2006.

[23] S. Sanchez-Cortes, C. Domingo, J. V. Garcia-Ramos, and J. A. Aznarez, Surface-enhanced vibrational study (SEIR and SERS) of dithiocarbamate pesticides on gold films, Langmuir, vol. 17 (4), pp. 1157-1162, 2001.

[24] J. S. Kang, S. Y. Hwang, C. J. Lee, and M. S. Lee, SERS of dithiocarbamate pesticides adsorbed on silver surface; thiram, Bull. Korean Chem. Soc., vol. 23 (11), pp. 1604-1610, 2002.

[25] Y. Zhao, W. Perez-Segarra, Q. Shi, and A. Wei, Dithiocarbamate assembly on gold, J. Am. Chem. Soc., vol. 127, 7328, 2005.

[26] C. Dimingo, V. Resta, S. Sanchez-Cortes, J. V. Garcia-Ramos, and J. Gonzalo, Pulsed laser deposited Au nanoparticles as substrates for surface-enhanced vibrational spectroscopy, J. of Phys. Chem., vol. C 111 (23), pp. 8149-8152, 2007.

[27] Y. Zhao, J. N. Newton, J. Liu, and A. Wei, Dithiocarbamate-coated SERS substrates: sensitivity gain by partial surface passivation, Langmuir, vol. 25 (24), pp. 13833-13839, 2009.

[28] B. Saute, R. Premasiri, L. Ziegler, and R. Narayanan, Gold nanorods as surface enhanced Raman spectroscopy substrates for sensitive and selective detection of ultra-low levels of dithiocarbamate pesticides, Analyst, vol. 137 (21), pp. 5082-5087, 2012.

[29] S. Sanhez-Cortes, M. Vasina, and O. Francioso, Raman and surface-enhanced Raman spectroscopy of dithiocarbamate fungicides, Vibrational Spectroscopy, vol. 17 (2), pp. 133-144, 1998.

[30] M. L. Nicholas, D. L. Powel, T. R. Williams, and R. H. Bromund, Reference Raman spectra of DDT and five structurally related pesticides and of five pesticides containing the norbornen group, J. of the AOC, vol. 59, 1, pp. 197-208, 1976.